6510 *Macromolecules* **2009**, *42*, 6510–6518
DOI: 10.1021/ma900906t

Macromolecules
ARTICLE

Poly(oligothiophene-*alt*-benzothiadiazole)s: Tuning the Structures of Oligothiophene Units toward High-Mobility "Black" Conjugated Polymers

Wei Yue,[†,‡] Yun Zhao,[†,‡] Hongkun Tian,[†] De Song,[†,‡] Zhiyuan Xie,[†] Donghang Yan,[†] Yanhou Geng,*[,†] and Fosong Wang[†]

[†]*State Key Laboratory of Polymer Physics and Chemistry, Changchun Institute of Applied Chemistry, Chinese Academy of Sciences, Changchun 130022, P. R. China, and* [‡]*Graduate School of Chinese Academy of Sciences, Beijing 100049, P. R. China*

Received April 26, 2009; Revised Manuscript Received July 3, 2009

ABSTRACT: A series of donor−acceptor low-bandgap conjugated polymers, i.e., **PT*n*BT** (n = 2−6), composed of alternating oligothiophene (OTh) and 2,1,3-benzothiadiazole (BT) units were synthesized by Stille cross-coupling polymerization. The number of thiophene rings in OTh units, that is n, was tuned from 2 to 6. All these polymers display two absorption bands in both solutions and films with absorption maxima depending on n. From solution to film, absorption spectra of the polymers exhibit a noticeable red shift. Both high- and low-energy absorption bands of **PT5BT** and **PT6BT** films locate in the visible region, which are at 468 and 662 nm for **PT5BT** and 494 and 657 nm for **PT6BT**. Consequently, their absorption spectra cover the region between 400 and 800 nm, and their optical bandgaps are 1.56 and 1.52 eV, respectively, which renders them "black" polymers. Moreover, **PT5BT** and **PT6BT** can form highly ordered thin films with field-effect mobilities up to 2.46×10^{-2} and 1.40×10^{-2} $cm^2\ V^{-1}\ s^{-1}$, respectively. Bulk-heterojunction polymer solar cells (PSCs) fabricated with these polymers as the donor materials and 1-(3-methoxycarbonyl)propyl-1-phenyl-[6,6]-C-61 (PCBM) as the acceptor material exhibited power conversion efficiencies (PCEs) of 0.93−2.23%. PSCs based on the high-mobility "black" polymer **PT6BT** showed the best device performance with a PCE of 2.23%. Our results provide a rational strategy for design and synthesis of high-mobility low-bandgap conjugated polymers with broad absorption range.

Introduction

Many conjugated polymers have been developed for a variety of applications, such as polymer light-emitting diodes (PLEDs),[1] polymer solar cells (PSCs),[2−4] and organic thin-film transistors (OTFTs).[5] Particularly, their solution processability allows low-cost fabrication process for producing lightweight, large area, and flexible optoelectronic devices.

High-mobility low-bandgap conjugated polymers, which are capable of harvesting solar energy and transporting excitons and charge carriers efficiently, have attracted great attention in the past several years for their application in PSCs.[2,3] It is believed that an ideal conjugated polymer for PSCs should have a mobility $> 10^{-3}$ $cm^2\ V^{-1}\ s^{-1}$ and a bandgap around 1.5 eV (corresponding to an absorption edge of ~800 nm).[3] To make low-bandgap conjugated polymers, the most successful approach involves incorporation of alternating electron-rich and electron-deficient aromatic units into the polymer chain.[6−38] The resulting polymers are so-called donor (D)−acceptor (A) conjugated polymers. With this molecular design concept, several high-mobility low-bandgap conjugated polymers with promising PSC properties have been demonstrated.[7,10,15,16,26,34,35] On the other hand, it has been proved that expanding the absorption range of the polymers can improve PSC performance due to more efficient harvesting of solar energy.[39−41] Therefore, high-mobility low-bandgap conjugated polymers with broad absorption spectra are very attractive for PSC application. However, design and synthesis of conjugated polymers with low bandgap, broad absorption spectrum, and high mobility all three properties are rather difficult.[27,33]

One possible approach to develop D−A conjugated polymers with broad absorption spectrum is to tailor the structures of D- or A-units to endow the polymers multiple intense absorption bands in visible region. For example, Reyonlds et al. recently reported D−A conjugated polymers composed of alternating oligothiophene (OTh) and 2,1,3-benzothiadiazole (BT) units, which exhibited promising electrochromic properties.[42] Most interestingly, these polymers exhibit two-band absorption spectra with absorption maxima depending on the structures of OTh units. Meanwhile, many thiophene-based conjugated polymers exhibit very high mobility.[43−46] Accordingly, we postulate that it is possible to obtain high-mobility low-bandgap polymers with absorption covering the whole visible region (400−800 nm), which means "black" polymers, by integrating appropriate OTh and BT units into polymer chains.

In the current paper, we report our effort on design and synthesis of aforementioned "black" conjugated polymers, which are named as **PT*n*BT**. The number of thiophene units in OThs was tuned from 2 to 6 to investigate the effect of the length of the OTh units and the orientation of alkyls on the properties of the polymers.

Experimental Section

Materials. Tetrahydrofuran (THF) and toluene were distilled over sodium/benzophenone. Chloroform ($CHCl_3$) and *N*,*N*-dimethylformamide (DMF) were purified by refluxing with calcium hydride and then distilled. Other reagents were used as received without further purification. Intermediates 3-dodecylthiophene (**9**),[47] 2-bromo-3-dodecylthiophene (**3**),[47]

*Corresponding author. E-mail: yhgeng@ciac.jl.cn.

 Published on Web 07/20/2009

4,7-dibromo-2,1,3-benzothiadiazole (**11**),[20] 2,5-bis(tri-*n*-butylstannyl)thiophene (**4**),[48] 2,5-bis(trimethylstannyl)thiophene (**14**),[49] 3,3′-didodecyl-2,2′-bithiophene (**1**),[50] and 3,3‴-didodecyl-2,2′:5′,2″:5″,2‴-quaterthiophene (**7**)[51] were prepared according to literature procedures.

5,5′-Bis(trimethylstannyl)-3,3′-didodecyl-2,2′-bithiophene (2). Into a solution of **1** (1.40 g, 2.78 mmol) in THF (30 mL) was added *n*-BuLi (2.40 mL, 6.00 mmol, 2.5 M in hexane) at −20 °C. The mixture was maintained at this temperature for 30 min, warmed to room temperature for another 30 min, and then recooled to −20 °C. Trimethyltin chloride (1.17 g, 5.85 mmol) was added at once. The mixture was stirred overnight at room temperature and poured into water for extraction with diethyl ether (3 × 50 mL). The combined organic layers were washed with brine (2 × 100 mL) and dried over $MgSO_4$. After the solvent had been removed under reduced pressure, the residue was purified by recrystallization from acetone to afford **2** as a white powder in a yield of 86.0% (1.98 g). ^{1}H NMR ($CDCl_3$, 300 MHz): δ (ppm) 7.01 (s, 2 H), 2.50 (t, J = 7.5 Hz, 4 H), 1.53−1.57 (m, 4 H), 1.18−1.28 (m, 36 H), 0.87 (t, J = 6.3 Hz, 6 H), 0.36 (s, 18 H). ^{13}C NMR ($CDCl_3$, 75 MHz): δ (ppm) 142.8, 137.3, 136.8, 135.2, 31.94, 30.93, 29.68, 29.59, 29.45, 29.37, 28.75, 22.69, 14.10, −8.25. Anal. Calcd for $C_{38}H_{70}S_2Sn_2$ (%): C, 55.29; H, 8.52. Found (%): C, 55.57; H, 8.77.

3,3″-Didodecyl-2,2′:5′,2″-terthiophene (5). A mixture of 2,5-bis(tri-*n*-butylstannyl)thiophene (**4**, 3.16 g, 4.80 mmol) and 2-bromo-3-dodecylthiophene (**3**, 3.31 g, 10.0 mmol) was deaerated three times with argon, and then DMF (40 mL) was added. After tetrakis(triphenylphosphine)palladium ($Pd(PPh_3)_4$, 46.0 mg, 4.00×10^{-2} mmol) was added, the reaction mixture was stirred for 48 h at 90 °C under dark. After cooling, the reaction mixture was poured into water (200 mL) for extraction with diethyl ether (3 × 100 mL). The combined organic layers were washed with brine (3×100 mL) and subsequently dried over $MgSO_4$. After the solvent had been removed, the residue was purified by column chromatography on silica gel to afford **5** as a light yellow liquid with a yield of 78.6% (1.84 g). ^{1}H NMR ($CDCl_3$, 300 MHz): δ (ppm) 7.21 (d, J = 5.2 Hz, 2 H), 7.09 (s, 2 H), 6.97 (d, J = 5.2 Hz, 2 H), 2.82 (t, J = 7.7 Hz, 4 H), 1.64−1.71 (m, 4 H), 1.29−1.37 (m, 36 H), 0.92 (t, J = 6.4 Hz, 6 H). ^{13}C NMR ($CDCl_3$, 75 MHz): δ (ppm) 139.7, 136.1, 130.5, 130.1, 126.0, 123.7, 31.99, 30.80, 29.73, 29.64, 29.56, 29.42, 29.36, 22.75, 14.16.

5,5″-Bis(trimethylstannyl)-3,3″-didodecyl-2,2′:5′,2″-terthiophene (6). Compound **6** was synthesized following the procedure for preparation of **2** as a yellow liquid in a yield of 59.7% (1.39 g). ^{1}H NMR ($CDCl_3$, 300 MHz): δ (ppm) 7.02 (s, 2 H), 6.98 (s, 2 H), 2.78 (t, J = 7.5 Hz, 4 H), 1.60−1.69 (m, 4 H), 1.24−1.37 (m, 36 H), 0.87 (t, J = 6.3 Hz, 6 H), 0.37 (s, 18 H). ^{13}C NMR ($CDCl_3$, 75 MHz): δ (ppm) 141.0, 140.7, 140.5, 138.5, 136.6, 136.3, 125.7, 32.18, 31.11, 29.93, 29.73, 29.61, 29.46, 22.93, 14.36, −8.10.

5,5‴-Bis(trimethylstannyl)-3,3‴-didodecyl-2,2′:5′,2″:5″,2‴-quaterthiophene (8). Compound **8** was synthesized following the procedure for preparation of **2** as a yellow solid in a yield of 89.7% (4.01 g). ^{1}H NMR ($CDCl_3$, 300 MHz): δ (ppm) 7.13−7.16 (m, 2 H), 6.99−7.09 (m, 4 H), 2.82 (t, J = 7.8 Hz, 4 H), 1.67−1.75 (m, 4 H), 1.29−1.38 (m, 36 H), 0.89 (t, J = 6.9 Hz, 6 H), 0.42 (s, 18 H). ^{13}C NMR ($CDCl_3$, 75 MHz): δ (ppm) 141.0, 138.4, 136.7, 135.6, 126.0, 123.8, 31.94, 30.80, 29.69, 29.47, 29.37, 29.22, 22.70, 14.11, −8.24. Anal. Calcd for $C_{46}H_{74}S_4Sn_2$ (%): C, 55.65; H, 7.51. Found (%): C, 56.01; H, 7.96.

2-(4-Dodecylthien-2-yl)-4,4,5,5-tetramethyl-[1,3,2]dioxaborolane (10). 2,2,6,6-Tetramethylpiperidine (HTMP, 3.00 g, 20.8 mmol) was dissolved in anhydrous THF (40 mL) in a 250 mL round-bottom flask. The mixture was cooled to −78 °C, and *n*-BuLi (7.90 mL, 19.8 mmol, 2.5 M in hexane) was added dropwise. The mixture was stirred at this temperature for 1 h. Then the solution of 3-dodecylthiophene (**9**, 4.54 g, 18.0 mmol) in THF (15 mL) was added dropwise, and the mixture was stirred for another 1 h. After triisopropyl borate (6.77 g, 8.32 mmol) was added, the mixture was stirred at −78 °C for 30 min and then overnight at room temperature. Hydrochloric acid (2 M, 60 mL) was added into the mixture, the organic phase was separated, and the aqueous layer was extracted with diethyl ether (3 × 100 mL). The combined organic layers were washed with brine (3 × 100 mL) and subsequently dried over $MgSO_4$ in the presence of 2,3-dimethyl-2,3-butandiol (6.38 g, 54.0 mmol) for 1 day. After the solvent was evaporated, the residue was purified by column chromatography on silica gel with petroleum ether/dichloromethane (4:1) as eluent to afford **10** as a colorless liquid in a yield of 68.7% (4.68 g). ^{1}H NMR ($CDCl_3$, 300 MHz): δ (ppm) 7.93 (d, J = 0.96 Hz, 1 H), 7.24 (d, J = 0.6 Hz, 1 H), 2.65 (t, J = 7.5 Hz, 2 H), 1.64−1.71 (m, 2 H), 1.37 (s, 12 H), 1.29−1.34 (m, 18 H), 0.92 (t, J = 6.4 Hz, 3 H). ^{13}C NMR ($CDCl_3$, 75 MHz): δ (ppm) 145.1, 138.9, 127.9, 84.33, 32.34, 31.08, 30.39, 30.08, 29.99, 29.88, 29.77, 29.73, 25.16, 23.10, 14.52.

4,7-Bis(4-dodecylthien-2-yl)-2,1,3-benzothiadiazole (12). 10 (0.80 g, 2.11 mmol), 4,7-dibromo-2,1,3-benzothiadiazole (**11**, 0.27 g, 0.92 mmol), and anhydrous Na_2CO_3 (0.90 g, 8.46 mmol) were added into a 100 mL Schlenk tube. The mixture was degassed with argon, and then oxygen-free water (4.20 mL) and the solution of $Pd(PPh_3)_4$ (10.6 mg, 9.2×10^{-3} mmol) in anhydrous THF (10.5 mL) were added. The mixture was heated at 85 °C for 60 h under dark. Water (30 mL) was added, the organic phase was separated and the aqueous layer was extracted with dichloromethane (4 × 50 mL). The combined organic layers were washed with brine (2 × 100 mL) and subsequently dried over $MgSO_4$. After the solvent had been removed under reduced pressure, the residue was purified by column chromatography on silica gel with petroleum ether/dichloromethane (6:1) as eluent to afford **12** as an orange solid in a yield of 94.9% (0.56 g). ^{1}H NMR ($CDCl_3$, 300 MHz): δ (ppm) 7.97 (d, J = 1.3 Hz, 2 H), 7.82 (s, 2 H), 7.03 (d, J = 0.7 Hz, 2 H), 2.68 (t, J = 7.5 Hz, 4 H), 1.64−1.74 (m, 4 H), 1.25−1.34 (m, 36 H), 0.87 (t, J = 6.3 Hz, 6 H). ^{13}C NMR ($CDCl_3$, 75 MHz): δ (ppm) 152.6, 144.3, 139.0, 129.0, 126.0, 125.5, 121.5, 31.94, 30.68, 30.52, 29.70, 29.52, 29.40, 22.71, 14.12. Anal. Calcd for $C_{38}H_{56}N_2S_3$ (%): C, 71.64; H, 8.86; N, 4.40. Found (%): C, 71.54; H, 8.99; N, 4.74.

4,7-Bis(5-bromo-4-dodecylthien-2-yl)-2,1,3-benzothiadiazole (13). A solution of *N*-bromosuccinimide (NBS) (0.24 g, 1.32 mmol) in $CHCl_3$ (10 mL) and DMF (4 mL) was added dropwise to an ice-cooled solution of **12** (0.40 g, 0.63 mmol) in $CHCl_3$ (30 mL). After addition, the mixture was stirred overnight at room temperature, and then CH_2Cl_2 (200 mL) was added. The solution was washed with brine (2 × 150 mL) and subsequently dried over $MgSO_4$. After the solvent had been removed under reduced pressure, the residue was purified by column chromatography on silica gel with petroleum ether/dichloromethane (4:1) as eluent to afford **13** as a red solid in a yield of 90.0% (0.45 g). ^{1}H NMR ($CDCl_3$, 300 MHz): δ (ppm) 7.76 (s, 2 H), 7.74 (s, 2 H), 2.63 (t, 4 H, J = 7.5 Hz), 1.61−1.68 (m, 4 H), 1.25−1.35 (m, 36 H), 0.86 (t, 6 H, J = 6.3 Hz). ^{13}C NMR ($CDCl_3$, 75 MHz): δ (ppm) 152.5, 143.4, 138.9, 128.4, 125.5, 125.0, 112.0, 32.33, 30.08, 29.86, 29.76, 29.73, 23.09, 14.51. Anal. Calcd for $C_{38}H_{54}Br_2N_2S_3$ (%): C, 57.42; H, 6.85; N, 3.52. Found (%): C, 57.59; H, 7.07; N, 3.78.

Poly(3,3′-didodecyl-2,2′-bithiophene-*alt*-2,1,3-benzothiadiazole) (PT2BT). A mixture of **2** (0.56 g, 0.67 mmol), **11** (0.19 g, 0.66 mmol), tris(dibenzylideneacetone)dipalladium (Pd_2dba_3, 12.1 mg, 1.30×10^{-2} mmol), and PPh_3 (27.7 mg, 0.11 mmol) was degassed with argon, and then toluene (24 mL) was added. The mixture was further purged with argon for 10 min and heated to 120 °C for 48 h. Then 4-bromotoluene (22.9 mg, 0.13 mmol) was added, and the reaction was continued for another 12 h. The polymer was precipitated in methanol. The crude polymer was collected by filtration and then extracted on a Soxhlet's extractor with acetone, hexane, and chloroform in succession. The final product was obtained by precipitating the chloroform solution in methanol as a dark red solid in a yield of

95.2% (400 mg). GPC: M_n = 40 700; PDI = 1.43. ^{1}H NMR (400 MHz, $C_2D_2Cl_4$, 353 K): δ (ppm) 8.08 (s, 2 H), 7.89 (s, 2 H), 2.72 (s, 4 H), 1.73 (s, 4 H), 1.23−1.39 (m, 36 H), 0.86 (s, 6H). Anal. Calcd for $C_{38}H_{56}N_2S_3$ (%): C, 71.64; H, 8.86; N, 4.40. Found (%): C, 71.88; H, 8.79; N, 3.99.

Poly(3,3′′-didodecyl-2,2′:5′,2′′-terthiophene-*alt*-2,1,3-benzothiadiazole) (PT3BT). PT3BT was synthesized following the procedure for preparation of **PT2BT** as a dark blue solid in a yield of 94.1% (320 mg). GPC: M_n = 25 800; PDI = 1.87. ^{1}H NMR (400 MHz, $C_2D_2Cl_4$, 353 K): δ (ppm) 7.99 (s, 2 H), 7.83 (s, 2 H), 7.23 (s, 2 H), 2.90 (s, 4 H), 1.79 (s, 4 H), 1.27−1.46 (m, 36 H), 0.87 (s, 6H). Anal. Calcd for $C_{42}H_{58}N_2S_4$ (%): C, 70.14; H, 8.13; N, 3.90. Found (%): C, 69.56; H, 7.88; N, 3.67.

Poly(3,3′,3′′,3′′′-tetradodecyl-2,5′:2′,2′′:5′′,2′′′-quaterthiophene-*alt*-2,1,3-bezothiadiazole) (PT4BT). PT4BT was synthesized following the procedure for preparation of **PT2BT** as a purple-brown solid in a yield of 78.0% (390 mg). GPC: M_n = 24 000; PDI = 1.72. ^{1}H NMR (400 MHz, $C_2D_2Cl_4$, 353 K): δ (ppm) 7.99 (s, 2 H), 7.84 (s, 2 H), 7.14 (s, 2 H), 2.90 (s, 4 H), 2.63 (s, 4 H), 1.79 (s, 4 H), 1.79 (s, 4 H), 1.66 (s, 4 H), 1.27−1.47 (m, 72 H), 0.86 (s, 12H). Anal. Calcd for $C_{70}H_{108}N_2S_5$ (%): C, 73.88; H, 9.57; N, 2.46. Found (%): C, 73.05; H, 9.90; N, 2.08.

Poly(3,3′,3′′′,3′′′′-tetradodecyl-2,5′:2′,2′′:5′′,2′′′:5′′′,2′′′′-pentathiophene-*alt*-2,1,3-benzothiadiazole) (PT5BT). PT5BT was synthesized following the procedure for preparation of **PT2BT** as a black solid in a yield of 92.0% (340 mg). GPC: M_n = 13 700; PDI = 1.38. ^{1}H NMR (400 MHz, $C_2D_2Cl_4$, 353 K): δ (ppm) 7.98 (s, 2 H), 7.83 (s, 2 H), 7.14 (s, 2 H), 7.10 (s, 2 H), 2.84−2.89 (m, 8 H), 1.76 (s, 8 H), 1.27−1.46 (m, 72 H), 0.87 (s, 6H). Anal. Calcd for $C_{74}H_{110}N_2S_6$ (%): C, 72.85; H, 9.09; N, 2.30. Found (%): C, 73.16; H, 9.32; N, 2.00.

Poly(3,3′,3′′′′,3′′′′′-tetradodecyl-2,5′:2′,2′′:5′′,2′′′:5′′′,2′′′′:5′′′′,-2′′′′′-hexathiophene-*alt*-2,1,3-benzothiadiazole) (PT6BT). PT6BT was synthesized following the procedure for preparation of **PT2BT** as a black solid in a yield of 87.2% (410 mg). GPC: M_n = 7200; PDI = 1.24. ^{1}H NMR (400 MHz, $C_2D_2Cl_4$, 353 K): δ (ppm) 7.98 (s, 2 H), 7.83 (s, 2 H), 7.17 (s, 2 H), 7.10 (s, 2 H), 2.83−2.89 (m, 8 H), 1.74−1.79 (s, 8 H), 1.28−1.44 (m, 72 H), 0.88 (s, 6H). Anal. Calcd for $C_{78}H_{112}N_2S_7$ (%): C, 71.94; H, 8.67; N, 2.15. Found (%): C, 71.06; H, 8.83; N, 1.79.

Measurements. ^{1}H NMR and ^{13}C NMR spectra were recorded on a Bruker AV 300 or a AV 400 spectrometer. Elemental analysis was performed on a VarioEL elemental analysis system. Gel permeation chromatography (GPC) measurements were conducted on a GPC system equipped with Waters HT4 and HT3 column assembly and a Waters 2414 interferometric refractometer using polystyrene as standard and $CHCl_3$ as the eluent. Differential scanning calorimetry (DSC) was run on a TA Q100 thermal analyzer at heating/cooling rates of 10 °C min^{-1} under N_2 flow. Thermogravimetric analysis (TGA) was carried out on a Perkin-Elmer TGA7 thermogravimetric analyzer at a heating rate of 10 °C min^{-1} under N_2 flow. UV−vis absorption spectra were recorded on a Shimadzu UV-3600 UV−vis−NIR spectrometer. Cyclic voltammetry (CV) was performed on a CHI660a electrochemical analyzer with a three-electrode cell in a solution of 0.1 mol L^{-1} Bu_4NPF_6 in acetonitrile at a scan rate of 100 mV s^{-1}. A glassy carbon electrode with a diameter of 10 mm, a Pt wire, and a saturated calomel electrode were used as the working, counter, and reference electrodes, respectively. The potential was calibrated against the ferrocene/ferrocenium couple (Fc/Fc^+). The highest occupied molecular orbital (HOMO) and the lowest unoccupied molecular orbital (LUMO) energy levels were estimated by the equations HOMO = $-(4.80 + E_{ox}^{onset})$ and LUMO = $-(4.80 + E_{red}^{onset})$.[52] Thin-film X-ray diffraction (XRD) was recorded on a Bruker D8 Discover thin-film diffractometer with Cu Kα radiation (λ = 1.540 56 Å) operated at 40 keV and 40 mA. Atomic force microscopy (AFM) measurements were performed in tapping mode on a SPA400HV instrument with a SPI 3800 controller (Seiko Instruments).

OTFT Device Fabrication and Characterization. OTFTs were fabricated in a bottom gate, top contact configuration on heavily doped n-type silicon wafers covered with 300 nm thick thermally grown silicon dioxide (SiO_2) (capacitance: 10 nF cm^{-2}). The wafer was immersed in a 10 mmol L^{-1} solution of octadecyltrichlorosilane (OTS-18) in toluene for 45 min, followed by rinsing with toluene. The semiconductor layer of 30 nm was deposited on top of the OTS-18-modified SiO_2 surface by spin-casting the chlorobenzene solution of the polymer with a concentration of 7 mg/mL at 1000 rpm. Finally, gold (40 nm) source and drain electrodes were deposited through a shadow mask with a channel width (W) of 4000 μm and a channel length (L) of 150 μm. The electrical measurements were performed with two Keithley 236 source/measure units at room temperature in ambient atmosphere.

Photovoltaic Device Fabrication and Characterization. PSCs were fabricated with the device structure of ITO/poly(3,4-ethylene dioxythiophene):poly(styrenesulfonate) (PEDOT:PSS)/polymer:PCBM/LiF/Al. The ITO glass was precleaned and modified by a 30 nm PEDOT:PSS (Baytron P4083). Then the active layer with a thickness of 90−110 nm was prepared by spin-coating the chlorobenzene solution of the polymer and PCBM (1:3, w/w) on the substrate. Finally, LiF/Al cathode was deposited at a vacuum level of 4×10^{-4} Pa. The thicknesses of the LiF and Al layers are 1 and 100 nm, respectively. The effective area of the unit cell is 12 mm^2. The current−voltage ($I-V$) measurement of the devices was conducted on a computer-controlled Keithley 236 source measure unit. A xenon lamp (500 W) with AM 1.5 filter was used as the white light source, and the optical power at the sample was 100 mW/cm^2. The external quantum efficiency (EQE) was measured using a model SR830 DSP lock-in amplifier coupled with SBP500 monochromator, DSC102 data acquisition system, and model SR540 chopper controller. The light intensity at each wavelength was calibrated with a standard single-crystal Si photodiode.

Results and Discussion

Design Concept for PT*n*BT. The structures of the conjugated polymers in the current paper are depicted in Figure 1. For ease of discussion, the polymers are abbreviated as **PT*n*BT**, in which **T*n*** and **BT** represent oligothiophene (OTh) and 2,1,3-benzothiadiazole (BT) units, respectively. The number of thiophene in the OTh units, that is n, is from 2 to 6. Polymers **PT3BT**, **PT5BT**, and **PT6BT** all involve OTh units with unsubstituted thiophene rings in center for releasing steric hindrance between neighboring thiophene rings. From references, polythiophenes comprising similar OTh units exhibit high mobility.[43,45,46] We expect that this structural design can afford low-bandgap conjugated polymers with high mobility. Meanwhile, extension of the length of the OTh units can endow the polymers an additional absorption band for expanding their absorption breadth.[42]

Synthesis and Characterization. Scheme 1 shows the synthesis of the monomers and polymers. Organotin reagents **2**, **6**, and **8** were synthesized in yields of 86%, 60%, and 90%, respectively, via deprotonation of corresponding OThs with *n*-BuLi followed by treatment with trimethyltin chloride. Compound **10** was synthesized in a modified procedure according to the literature.[53] 3-Dodecylthiophene (**9**) was first deprotonated with lithium 2,2,6,6-tetramethylpiperidide (LiTMP) followed by treatment with triisopropyl borate and 2,3-dimethyl-2,3-butandiol. After column chromatography, pure product was obtained as colorless oil with a moderate yield of 69%. The Suzuki coupling reaction between 4,7-dibromo-2,1,3-benzothiadiazole (**11**) and **10** afforded compound **12** in a yield of 95%. Bromination of **12** with *N*-bromosuccinimide (NBS) gave the dibrominated monomer **13** in a yield of 90%.

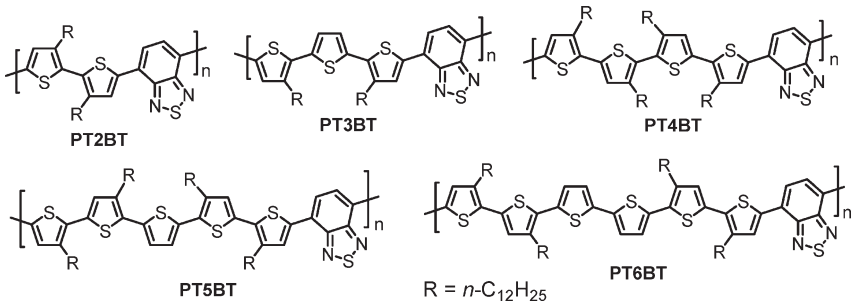

Figure 1. Chemical structures of **PT*n*BT**, in which *n* represents the number of thiophene in the oligothiophene (OTh) segments.

Scheme 1. Synthetic Route of Polymers PT*n*BT (n = 2−6)[a]

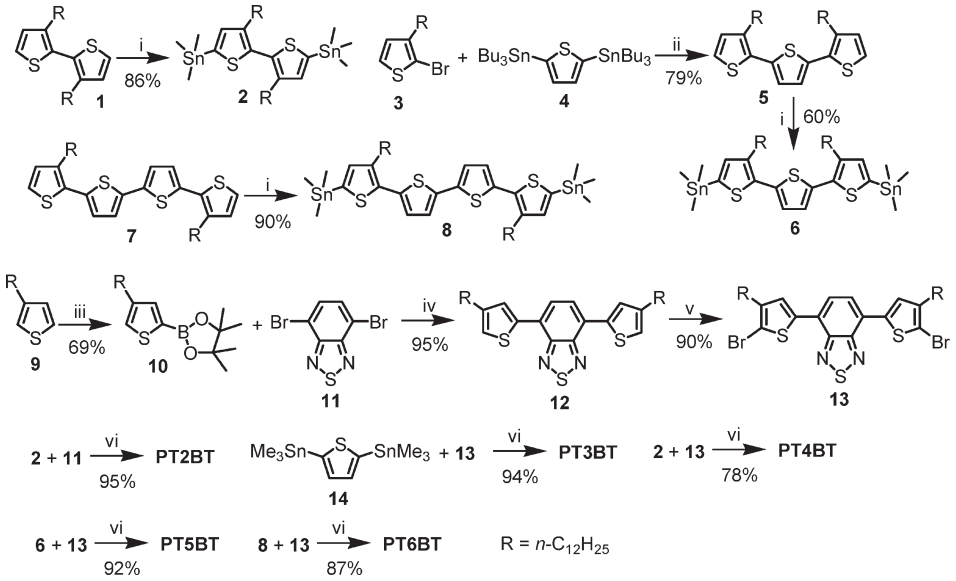

[a] (i) (1) *n*-BuLi, −20 °C to rt; (2) Me_3SnCl, −20 °C to rt. (ii) $Pd(PPh_3)_4$, DMF, 90 °C. (iii) (1) LiTMP, THF, −78 °C; (2) $B(O\text{-}i\text{-}C_3H_7)_3$, −78 °C to rt; (3) pinacol, rt. (iv) $Pd(PPh_3)_4$, Na_2CO_3, THF, H_2O, reflux. (v) NBS, $CHCl_3$, DMF, rt. (vi) Pd_2dba_3, PPh_3, toluene, 120 °C.

Polymers were synthesized by typical Stille cross-coupling reaction with Pd_2dba_3 as the catalyst and toluene as the solvent in high yields (78−95%).[9] The number-average molecular weights (M_ns) of these polymers determined by GPC against polystyrene standards in chloroform are in the range of 7200−40 700 g/mol with polydispersity indices (PDIs, PDI = weight-average molecular weight (M_w)/M_n) of 1.24−1.87, as shown in Table 1. The low molecular weight of **PT6BT** can be ascribed to its poor solubility in toluene. It should be pointed out that a polymer similar to **PT3BT** has been synthesized by Cao et al. with the different catalyst and organotin reagent. M_n of the polymer was only about 7400 g/mol.[19] Considering that the polymer with qauterthiophene **7** as the repeating unit exhibits high mobility,[45] the polymer composed of alternating **7** and BT units was also synthesized. However, its solubility is very poor in all tested solvents.

The chemical structures of the polymers were confirmed by ^{1}H NMR spectra and elemental analysis. Figure 2 shows the aromatic region ^{1}H NMR spectra of **PT4BT**, **PT5BT**, and **PT6BT** in $C_2D_2Cl_4$ at 353 K along with assignment. The ^{1}H NMR spectra of the polymers are in good agreement with the proposed structures. The singlet resonance at 7.98 ppm is assigned to the protons on BT units. The singlet resonances at 7.84 and 7.14 ppm are ascribed to the protons on the thiophene rings adjacent to BT units and the protons at position 3 on thiophene rings, respectively. The singlet resonance at 7.10 ppm is assigned to the protons at position 4 in **PT5BT** and positions 4 and 5 in **PT6BT**.

Table 1. Weight-Average Molecular Weights (M_ws), Number-Average Molecular Weights (M_ns), Polydispersity Indices (PDIs), and Decomposition Temperatures of PT*n*BT

polymer	M_w[a]	M_n[a]	PDI[a]	T_d[b] (°C)
PT2BT	58 200	40 700	1.43	417
PT3BT	48 300	25 800	1.87	385
PT4BT	41 300	24 000	1.72	381
PT5BT	18 900	13 700	1.38	409
PT6BT	8 900	7 200	1.24	416

[a] Determined by GPC with polystyrene as standard and $CHCl_3$ as eluent. [b] Temperature with 5% weight loss determined by TGA in N_2.

Thermal Properties. The thermal stability of **PT*n*BT** was characterized by thermogravimetric analysis (TGA) in N_2. As shown in Figure 3a and Table 1, all of the polymers are thermally stable with 5% weight-loss temperatures above 380 °C. The phase transitions of the polymers were investigated by differential scanning calorimetry (DSC). **PT2BT**, **PT3BT**, and **PT4BT** have no any phase transitions below decomposition temperature. In contrast, both **PT5BT** and **PT6BT** exhibit two endothermal transitions, as shown in Figure 3b. The transitions at the low and high temperatures should be ascribed to side chain melting and backbone melting, respectively.[54]

Photophysical Properties. Solution and film absorption spectra of the polymers were recorded, and related data are collected in Table 2. Figure 4a shows the solution spectra in $CHCl_3$ with a concentration of 1×10^{-5} M of repeating unit. All polymers have two absorption bands. As the length of the OTh units increases, the high-energy absorption maximum red-shifts from 332 nm for **PT2BT** to 368, 377, 410, and 430 nm for **PT3BT**, **PT4BT**, **PT5BT**, and **PT6BT**, respectively, and the low-energy absorption maximum red-shifts from 520 nm for **PT2BT** to 535, 536, 551, and 536 nm for **PT3BT**, **PT4BT**, **PT5BT**, and **PT6BT**, respectively. From **PT3BT** to **PT4BT**, only a negligible red shift was observed, which could be ascribed to the detrimental effect of the steric hindrance of the β-alkyl chains in central 3,3′-dialkyl-2,2′-bithiophene units on polymer conjugation. Compared to **PT5BT**, **PT6BT** exhibits a 15 nm blue shift of the low-energy absorption maximum, which may be related to its low molecular weight (the number of repeating unit is about 6 according to M_n), as shown in Table 1. Meanwhile, a long low-energy absorption tail in the spectrum of **PT6BT** is consistent with its low solubility. The red shift of the absorption maxima with increasing the length of OTh segments was also observed in thiophene/BT hybrid oligomers.[55] However, for a similar polymer system but with quinoxaline as the acceptor unit, it was found that the long wavelength absorption maxima were not significantly influenced by the length of OTh segments (605−614 nm).[56] This indicates that the polymers containing BT units have longer conjugation length.

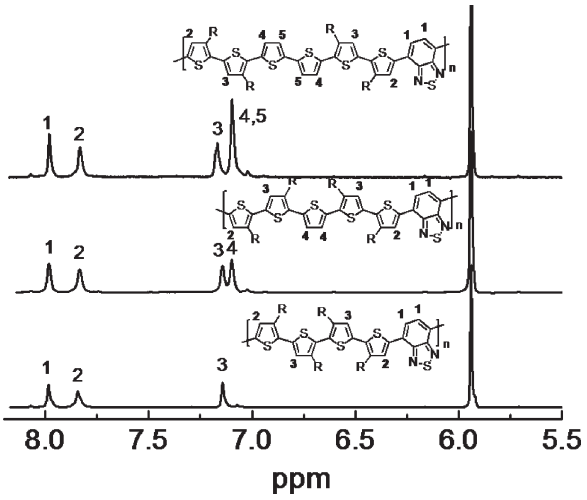

Figure 2. ^{1}H NMR spectra of **PT4BT**, **PT5BT**, and **PT6BT** in $C_2D_2Cl_4$ at 353 K.

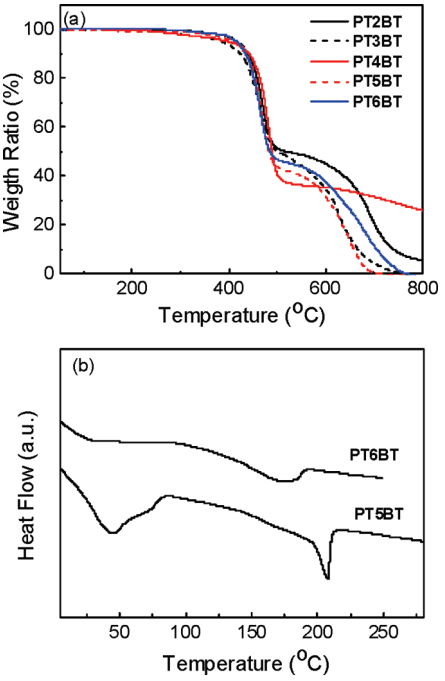

Figure 3. TGA plots of **PT*n*BT** (a) and the second DSC heating scans of **PT5BT** and **PT6BT** (b) with a heating rate of 10 °C/min under a N_2 atmosphere.

Film absorption spectra of the polymers are depicted in Figure 4b. Clearly, the chemical structures of OTh units have a strong effect on the property of the polymers in solid state. From solution to film, the spectra of **PT3BT**, **PT5BT**, and **PT6BT** exhibit a very large red shift, which are 58−64 and 97−121 nm for the high- and low-energy absorption bands, respectively, as shown in Table 2. This implies that the polymer chains adopt a more planar geometry and pack closely in solid state.[57,58] Most importantly, the absorption spectra of **PT5BT** and **PT6BT** cover the whole visible region (400−800 nm), meaning that they are "black" polymers. This feature is very attractive for high-performance PSC fabrication. In contrast, the red shifts of the spectra for **PT2BT** and **PT4BT** are much smaller (< 40 nm), as shown in Table 2. This is likely due to the steric repulsion between β-alkyl chains in 3,3′-dialkyl-2,2′-bithiophene units, which prohibits the polymers from forming more planar chains in solid state.[57] The optical bandgaps (E_g^{opt}) derived from the absorption edges of the film spectra were in the range of 1.52−1.97 eV. **PT3BT**, **PT5BT**, and **PT6BT** have nearly the same optical bandgaps of 1.52−1.58 eV, which are very close to the ideal bandgap for PSCs.[3] However, **PT2BT** and **PT4BT**, which involve steric repulsion in polymer chains, have relatively larger optical bandgaps of 1.97 and 1.72 eV, respectively.

Electrochemical Properties. The film electrochemical characteristics of the polymers were studied by cyclic voltammetry (CV) with Bu_4NPF_6 (0.1 M in acetonitrile) as the electrolyte at a scan rate of 100 mV s^{-1}. Depending on the structures of OTh segments, the oxidation onsets (E_{ox}^{onset}) of the polymers vary in the range of 0.08−0.79 V vs Fc/Fc^+ (Table 2), while the reduction onsets (E_{red}^{onset}) are very close (−1.57 to −1.70 V). The HOMO and LUMO energy levels

Table 2. Photophysical and Electrochemical Properties of PT*n*BT

polymer	λ_{max}^{abs}(nm) solution[a]	λ_{max}^{abs}(nm) film	E_{ox}^{onset} (V)/HOMO (eV)[b]	E_{red}^{onset} (V)/LUMO (eV)[b]	E_g^{ec} (eV)[c]	E_g^{opt} (eV)[d]
PT2BT	332, 520	344, 543	0.79/−5.59	−1.57/−3.23	2.36	1.97
PT3BT	368, 535	427, 632	0.23/−5.03	−1.63/−3.17	1.86	1.59
PT4BT	377, 536	393, 577	0.40/−5.20	−1.62/−3.18	2.02	1.72
PT5BT	410, 551	468, 662	0.08/−4.88	−1.70/−3.10	1.78	1.56
PT6BT	430, 536	494, 657	0.14/−4.94	−1.62/−3.18	1.76	1.52

[a] 1×10^{-5} M of the repeating unit in anhydrous chloroform. [b] All values are reported against Fc/Fc^+. [c] $E_g^{ec} = E_{ox}^{onset} - E_{red}^{onset}$ eV. [d] The optical bandgap was calculated according to the equation $E_g^{opt} = 1240/\lambda_{edge}$, where λ_{edge} is the onset value of the absorption spectrum in long wavelength region.

and electrochemical bandgaps (E_g^{ec}) of the polymers calculated from E_{ox}^{onset} and E_{red}^{onset} are listed in Table 2. **PT3BT**, **PT5BT**, and **PT6BT** have similar HOMO levels (−4.88 to −5.03 eV) and similar electrochemical bandgaps (1.76−1.86 eV). **PT2BT** and **PT4BT** have much lower HOMO levels, which are −5.59 and −5.20 eV, respectively. The HOMO level of regioregular poly(3-hexylthiophene) (**P3HT**) and the LUMO level of PCBM were also measured at the same condition, which are −4.86 and −3.75 eV, respectively. These values are identical to those reported in references measured in a similar method.[39,59]

Thin-Film XRD Analysis. Film nanostructures are very critical to the photophysical properties of thiophene-based conjugated polymers.[43] Figure 5 shows typical thin film XRD diagrams of **PT5BT** and **PT6BT**. At room temperature, pristine films of both polymers exhibit diffused diffraction peaks at $2\theta = 4.2°$ and 4.5°, corresponding to *d*-spacings of 21.0 and 19.6 Å for **PT5BT** and **PT6BT**, respectively. After annealing at 100 °C for 5 min, the diffraction peaks become stronger and sharper, and meanwhile the second-order diffraction peaks appear, indicating an enhanced film order upon annealing. This XRD feature implies that **PT5BT** and **PT6BT** polymer chains can form ordered edge-on lamellar nanostructures with alkyl chains arranged in a slightly interlocked or an end-to-end fashion.[43,54] No diffraction peaks were observed in the XRD diagrams of **PT2BT**, **PT3BT**, and **PT4BT** even after thermal annealing, suggesting that they only form amorphous films. These results are consistent with DSC studies, which also indicate that **PT5BT** and **PT6BT** can form ordered structures in the solid state.

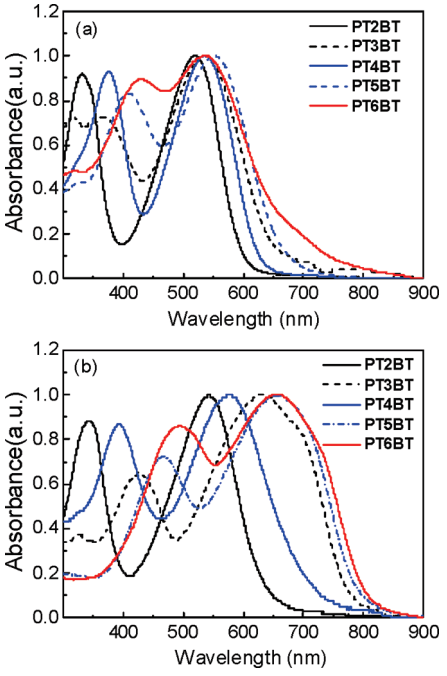

Figure 4. Solution (a, in $CHCl_3$ with a concentration of 1×10^{-5} M of repeating unit) and film (b) UV−vis absorption spectra of **PT*n*BT**.

OTFT Devices. Top-contact OTFT devices were fabricated on n-doped silicon substrates coated with 300 nm SiO_2 and modified with OTS-18 monolayer. OTFT devices based-on **PT5BT** and **PT6BT** show p-type characteristics and operate in an accumulation mode, but field-effect transport characteristics were not observed for **PT2BT**, **PT3BT**, and **PT4BT**, which is consistent with the low order of their films as indicated by XRD studies. Detail performance data of the devices are outlined in Table 3. OTFT devices based on pristine films exhibit hole mobilities of 4.58×10^{-3} and 3.65×10^{-3} cm^2 V^{-1} s^{-1} for **PT5BT** and **PT6BT**, respectively.

Consistent with XRD studies, it was found that thermal annealing could enhance device performance greatly. Figures 6 and 7 show the typical output and transfer characteristics of the devices based on **PT5BT** and **PT6BT** with thermal annealing of the films at 100 °C for 5 min. The current−voltage characteristics exhibit standard linear and saturation regions. The source−drain current (I_D) increases with an increase of the gate voltage (V_G). Mobilities (μ) for **PT5BT** and **PT6BT** are 2.46×10^{-2} and 1.40×10^{-2} cm^2 V^{-1} s^{-1}, respectively, as determined from the saturation regime.[60] These mobility values are comparable to those of the reference devices based on **P3HT** (Table 3).

Polymer Solar Cells (PSCs). PSCs with the device structure of ITO/PEDOT:PSS/polymer:PCBM(1:3, w/w)/LiF/Al were fabricated. Typical performance data of the devices are listed in Table 4, and corresponding current−voltage curves are illustrated in Figure 8a. More data for devices are included in Table S1 in the Supporting Information (SI), which support the reproducibility of device performance. Power conversion efficiencies (PCEs) of the polymers vary in the range of 0.93−2.23%. The large V_{oc} of the devices based on **PT2BT** and **PT4BT** is attributed to the big difference between the HOMO levels of the polymers and the LUMO level of PCBM, which is 1.45 and 1.84 eV for **PT2BT** and **PT4BT**, respectively. Compared to the previous reported quaterthiophene/BT-based polymer **PCPDTTBTT**,[61] **PT4BT** exhibits a much larger V_{oc}. For **PCPDTTBTT**, it should be noted that cyclopentadithiophene in the quaterthiophene segment could eliminate the steric effect of alkyl chains to render the polymer better conjugation, which

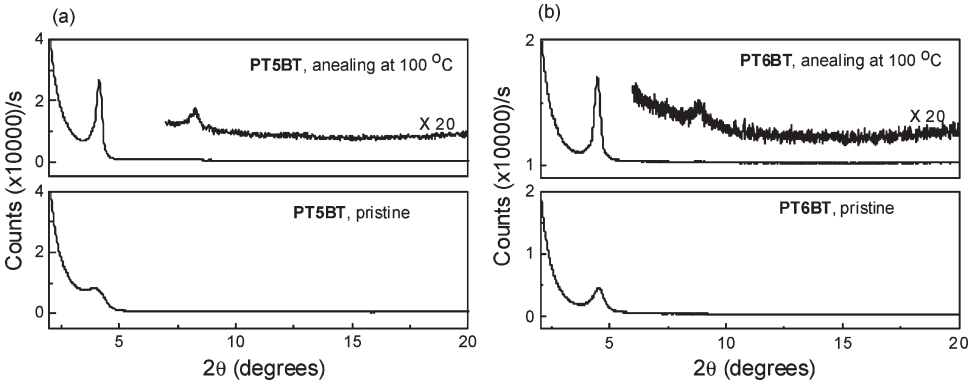

Figure 5. Thin-film X-ray diffraction (XRD) scans of **PT5BT** and **PT6BT** before and after thermal annealing at 100 °C for 5 min.

Table 3. OTFT Device Performance of PT*n*BT

	without annealing			with annealing		
	μ ($cm^2\ V^{-1}\ s^{-1}$)	I_{on}/I_{off}	V_T (V)	μ ($cm^2\ V^{-1}\ s^{-1}$)	I_{on}/I_{off}	V_T (V)
PT5BT	4.58×10^{-3}	4.5×10^2	−7.4	2.46×10^{-2}	3.1×10^3	−5.3
PT6BT	3.65×10^{-3}	1.1×10^3	−6.4	1.40×10^{-2}	1.9×10^3	−1.5
P3HT[a]	3.54×10^{-3}	1.2×10^3	−5.0	2.63×10^{-2}	1.0×10^4	−8.1

[a] M_w = 38 600 g/mol; PDI = 1.59; regioregularity ~ 97%.

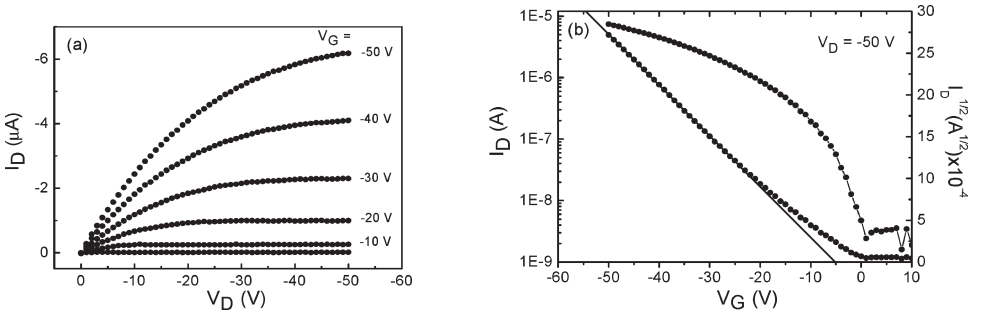

Figure 6. Output (a) and transfer (b) characteristics of a **PT5BT**-based OTFT device with annealing of the film at 100 °C for 5 min.

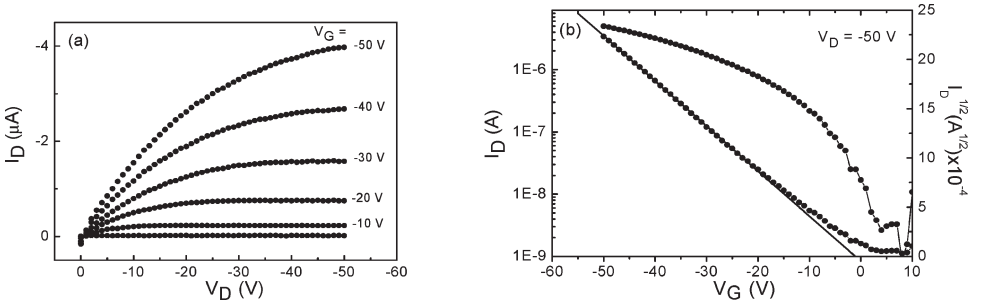

Figure 7. Output (a) and transfer (b) characteristics of a **PT6BT**-based OTFT device with annealing of the film at 100 °C for 5 min.

Table 4. PSC Performance of Polymers PT*n*BTs under Illumination of 100 mW/cm^2 White Light

polymer[a]	V_{oc} (V)	J_{sc} (mA/cm^2)	FF	PCE (%)
PT2BT	1.18	3.53	0.30	1.23
PT3BT	0.68	3.11	0.44	0.93
PT4BT	1.22	3.75	0.36	1.62
PT5BT	0.66	5.09	0.57	1.91
PT6BT	0.85	5.62	0.47	2.23

[a] Polymer:PCBM = 1:3 (w/w); the thickness of the active layer is 90−110 nm.

could raise its HOMO energy level and then result in a lower V_{oc}. **PT5BT** and **PT6BT** exhibit larger short circuit current (J_{sc}) and fill factor (FF), which are consistent with their higher mobilities and broad absorption spectra, as discussed above. **PT6BT** shows the best device performance with a V_{oc} of 0.85 V, a J_{sc} of 5.62 mA/cm^2, a FF of 0.47, and a PCE of 2.23%. Although **PT3BT** gave the worst device performance among the five polymers, the PCE value of 0.93% is still much higher than that (0.13%) of the similar polymer previously reported by Cao et al.[19] This difference can be ascribed to the much higher molecular weight of our polymer. As reported in reference, high molecular weight is one of the demanding factors for high-performance PSCs.[2a]

Depicted in Figure 8b,c are absorption spectra of the polymer/PCBM blends and external quantum efficiency (EQE) spectra of the corresponding PSCs. Both high- and low-energy absorption bands of the blends show a blue shift compared to those of the neat polymers, indicating the addition of PCBM can suppress the aggregation of the polymer chains. The photovoltaic response range of the devices is largely consistent with the absorption range of the blend. Particularly, **PT5BT** and **PT6BT** have response in the whole visible region, and their EQE values in the wavelength range from 350 to 800 nm are noticeably higher than other polymers. However, the low-energy absorption bands of **PT3BT**, **PT5BT**, and **PT6BT** contribute less to the device efficiency than high-energy bands while comparing the absorption and EQE spectra, probably due to the poor dissociation of low-energy excitons. This difference between EQE profiles and absorption spectra is likely related to the imperfect morphology of the films, although AFM images indicate that the films are uniform with the absence of large domains and crystals, as shown in Figure S6. Low EQE in the long-wavelength region was also observed in other low-bandgap polymer system. This problem can be solved by developing new acceptor materials, as reported by Wang et al.[62]

Conclusions

Five D−A conjugated polymers **PT*n*BT** (n = 2−6) comprising alternating OTh and BT units were synthesized by Stille coupling polymerization. Their chemical structures and properties were fully characterized. These polymers are thermally stable with decomposition temperatures beyond 380 °C. All polymers exhibit two-band absorption spectra with maxima depending on the length of OTh units. Film optical bandgaps of **PT3BT**, **PT5BT**, and **PT6BT** are 1.52−1.59 eV, while those for **PT2BT** and **PT4BT** are 1.97 and 1.72 eV, respectively. The absorption spectra of **PT5BT** and **PT6BT**, which contain quinquethiophene and

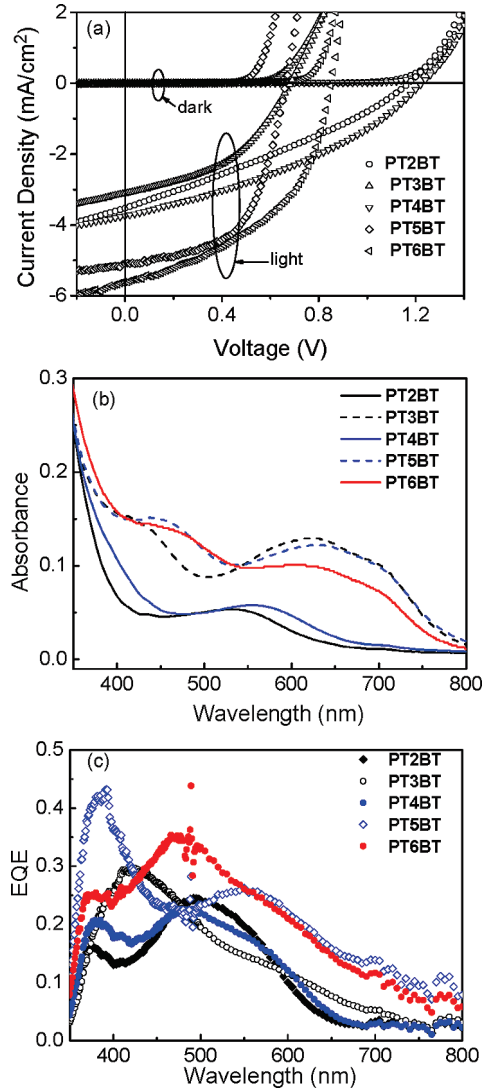

Figure 8. Current−voltage curves of PSCs in dark and under illumination of 100 mW/cm^2 white light (a) and UV−vis absorption spectra of **PT*n*BT**:PCBM (1:3) blend films (a) and EQE spectra (b) of PSCs.

sexithiophene segments, cover the whole visible region between 400 and 800 nm. Meanwhile, these two polymers can form highly ordered thin films for fabrication of OTFT devices with mobilities up to 2.46×10^{-2} and 1.40×10^{-2} cm^2 V^{-1} s^{-1}, respectively. PSCs fabricated with the blends of **PT*n*BT** and PCBM (polymer:PCBM = 1:3, w/w) gave PCEs of 0.93−2.23%. Better device performance was found for high mobility "black" polymers **PT5BT** and **PT6BT**. A V_{oc} of 0.85 V, a J_{sc} of 5.62 mA/cm^2, a FF of 0.47, and a PCE of 2.23% have been realized with **PT6BT**. Combination of high mobility, low bandgap, and broad absorption range make **PT5BT** and **PT6BT** very attractive optoelectronic materials.

Acknowledgment. This work is supported by NSFC (Nos. 20423003, 20521415, and 50833004), Science Fund for Creative Research Groups of NSFC (20621401), and Chinese Academy of Sciences (KJCX2-YW-M11).

Supporting Information Available: Cyclic voltammetry (CV) scans, temperature-dependent X-ray diffraction diagrams, AFM images of polymer/PCBM films, and detailed PSC device data of the polymers. This material is available free of charge via the Internet at http://pubs.acs.org.

References and Notes

(1) Grimsdale, A. C.; Chan, K. L.; Martin, R. E.; Jokisz, P. G.; Holmes, A. B. *Chem. Rev.* **2009**, *109*, 897.
(2) (a) Thompson, B. C.; Fréchet, J. M. J. *Angew. Chem., Int. Ed.* **2008**, *47*, 58. (b) Gunes, S.; Neugebauer, H.; Sariciftci, N. S. *Chem. Rev.* **2007**, *107*, 1324.
(3) Dennler, G.; Scharber, M. C.; Brabec, C. J. *Adv. Mater.* **2009**, *21*, 1323.
(4) (a) Chen, L.-M.; Hong, Z. R.; Li, G.; Yang, Y. *Adv. Mater.* **2009**, *21*, 1434. (b) Li, Y. F.; Zou, Y. P. *Adv. Mater.* **2008**, *20*, 2952.
(5) Allard, S.; Forster, M.; Souharce, B.; Thiem, H.; Scherf, U. *Angew. Chem., Int. Ed.* **2008**, *47*, 4070.
(6) van Mullekom, H. A. M.; Vekemans, J. A. J. M.; Havinga, E. E.; Meijer, E. W. *Mater. Sci. Eng, R.* **2001**, *32*, 1.
(7) Muhlbacher, D.; Scharber, M.; Morana, M.; Zhu, Z. G.; Waller, D.; Gaudiana, R.; Brabec, C. *Adv. Mater.* **2006**, *18*, 2884.
(8) Peet, J.; Kim, J. Y.; Coates, N. E.; Ma, W. L.; Moses, D.; Heeger, A. J.; Bazan, G. C. *Nat. Mater.* **2007**, *6*, 497.
(9) Zhu, Z. G.; Waller, D.; Gaudiana, R.; Morana, M.; Muhlbacher, D.; Scharber, M.; Brabec, C. *Macromolecules* **2007**, *40*, 1981.
(10) Blouin, N.; Michaud, A.; Leclerc, M. *Adv. Mater.* **2007**, *19*, 2295.
(11) Blouin, N.; Michaud, A.; Gendron, D.; Walkim, S.; Blair, E.; Neagu-Plesu, R.; Belletête, M.; Durocher, G.; Tao, Y.; Leclerc, M. *J. Am. Chem. Soc.* **2008**, *130*, 732.
(12) Zhou, E. J.; Nakamura, M.; Nishizawa, T.; Zhang, Y.; Wei, Q. S.; Tajima, K.; Yang, C. H.; Hashimoto, K. *Macromolecules* **2008**, *41*, 8302.
(13) Yue, W.; Zhao, Y.; Shao, S. Y.; Tian, H. K.; Xie, Z. Y.; Geng, Y. H.; Wang, F. S. *J. Mater. Chem.* **2009**, *19*, 2199.
(14) Hou, J. H.; Park, M.-H.; Zhang, S. Q.; Yao, Y.; Chen, L.-M.; Li, J.-H.; Yang, Y. *Macromolecules* **2008**, *41*, 6012.
(15) Hou, J. H.; Chen, H.-Y.; Zhang, S. Q.; Li, G.; Yang, Y. *J. Am. Chem. Soc.* **2008**, *130*, 16144.
(16) Wang, E. G.; Wang, L.; Lan, L. F.; Luo, C.; Zhuang, W. L.; Peng, J. B.; Cao, Y. *Appl. Phys. Lett.* **2008**, *92*, 033307.
(17) Xia, Y. J.; Wang, L.; Deng, X. Y.; Li, D. Y.; Zhu, X. H.; Cao, Y. *Appl. Phys. Lett.* **2006**, *89*, 081106.
(18) Zhou, Q. M.; Hou, Q.; Zheng, L. P.; Deng, X. Y.; Yu, G.; Cao, Y. *Appl. Phys. Lett.* **2004**, *84*, 1653.
(19) Xia, Y. J.; Deng, X. Y.; Wang, L.; Li, X. Z.; Zhu, X. H.; Cao, Y. *Macromol. Rapid Commun.* **2006**, *27*, 1260.
(20) Yang, R. Q.; Tian, R. Y.; Yan, J. G.; Zhang, Y.; Yang, J.; Hou, Q.; Yang, W.; Zhang, C.; Cao, Y. *Macromolecules* **2005**, *38*, 244.
(21) Liao, L.; Dai, L. M.; Smith, A.; Durstock, M.; Lu, J. P.; Ding, J. F.; Tao, Y. *Macromolecules* **2007**, *40*, 9406.
(22) Hou, L. J.; He, C.; Han, M. F.; Zhou, E. J.; Li, Y. F. *J. Polym. Sci., Part A: Polym. Chem.* **2007**, *45*, 3861.
(23) Brabec, C. J.; Winder, C.; Sariciftci, N. S.; Hummelen, J. C.; Dhanabalan, A.; van Hal, P. A.; Janssen, R. A. J. *Adv. Funct. Mater.* **2002**, *12*, 709.
(24) Svensson, M.; Zhang, F. L.; Veenstra, S. C.; Verhees, W. J. H.; Hummelen, J. C.; Kroon, J. M.; Inganas, O.; Andersson, M. R. *Adv. Mater.* **2003**, *15*, 988.
(25) Boudreault, P.-L. T.; Michaud, A.; Leclerc, M. *Macromol. Rapid Commun.* **2007**, *28*, 2176.
(26) Wong, W.-Y.; Wang, X.-Z.; He, Z.; Djurišić, A. B.; Yip, C.-T.; Cheung, K.-Y.; Wang, H.; Mak, C. S. K.; Chan, W.-K. *Nat. Mater.* **2007**, *6*, 521.
(27) Wu, P.-T.; Bull, T.; Kim, F. S.; Luscombe, C. K.; Jenekhe, S. A. *Macromolecules* **2009**, *42*, 671.
(28) Mei, J. G.; Heston, N. C.; Vasilyeva, S. V.; Reynolds, J. R. *Macromolecules* **2009**, *42*, 1482.
(29) Wu, P.-T.; Kim, F. S.; Champion, R. D.; Jenekhe, S. A. *Macromolecules* **2008**, *41*, 7021.
(30) Campos, L. M.; Tontcheva, A.; Gunes, S.; Sonmez, G.; Neugebauer, H.; Sariciftci, N. S.; Wudl, F. *Chem. Mater.* **2005**, *17*, 4031.
(31) Zhang, F. L.; Perzon, E.; Wang, X. J.; Mammo, W.; Andersson, M. R.; Inganas, O. *Adv. Funct. Mater.* **2005**, *15*, 745.
(32) Zhang, F. L.; Mammo, W.; Andersson, L. M.; Admassie, S.; Andersson, M. R.; Inganas, O. *Adv. Mater.* **2006**, *18*, 2169.
(33) Zoombelt, A. P.; Gilot, J.; Wienk, M. M.; Janssen, R. A. J. *Chem. Mater.* **2009**, *21*, 1663.
(34) Wienk, M. M.; Turbiez, M.; Gilot, J.; Janssen, R. A. *J. Adv. Mater.* **2008**, *20*, 2556.
(35) Zou, Y. P.; Gendron, D.; Badrou-Aich, R.; Najari, A.; Tao, Y.; Leclerc, M. *Macromolecules* **2009**, *42*, 2891.

(36) Zhan, X. W.; Tan, Z. A.; Domercq, B.; An, Z. S.; Zhang, X.; Barlow, S.; Li, Y. F.; Zhu, D. B.; Kippelen, B.; Marder, S. R. *J. Am. Chem. Soc.* **2007**, *129*, 7246.
(37) Thompson, B. C.; Kim, Y. G.; McCarley, T. D.; Reynolds, J. R. *J. Am. Chem. Soc.* **2006**, *128*, 12714.
(38) Colladet, K.; Fourier, S.; Cleij, T. J.; Lutsen, L.; Gelan, J.; Vanderzande, D.; Nguyen, L. H.; Neugebauer, H.; Sariciftci, S.; Aguirre, A.; Janssen, G.; Goovaerts, E. *Macromolecules* **2007**, *40*, 65.
(39) Hou, J. H.; Tan, Z. A.; Yan, Y.; He, Y. J.; Yang, C. H.; Li, Y. F. *J. Am. Chem. Soc.* **2006**, *128*, 4911.
(40) Hou, J. H.; Huo, L. J.; He, C.; Yang, C. H.; Li, Y. F. *Macromolecules* **2006**, *39*, 594.
(41) Hou, J. H.; Tan, Z. A.; He, Y. J.; Yang, C. H.; Li, Y. F. *Macromolecules* **2006**, *39*, 4657.
(42) Beaujuge, P. M.; Ellinger, S.; Reynolds, J. R. *Nat. Mater.* **2008**, *7*, 795.
(43) Ong, B. S.; Wu, Y. L.; Li, Y. N.; Liu, P.; Pan, H. L. *Chem.—Eur. J.* **2008**, *14*, 4766.
(44) Sirringhaus, H.; Brown, P. J.; Friend, R. H.; Nielsen, M. M.; Bechgaard, K.; Langeveld-Voss, B. M. W.; Spiering, A. J. H.; Janssen, R. A. J.; Meijer, E. W.; Herwig, P.; de Leeuw, D. M. *Nature* (*London*) **1999**, *401*, 685.
(45) Ong, B. S.; Wu, Y. L.; Liu, P.; Gardner, S. *J. Am. Chem. Soc.* **2004**, *126*, 3378.
(46) (a) Pokrop, R.; Verilhac, J.-M.; Gasior, A.; Wielgus, I.; Zagorska, M.; Travers, J.-P.; Pron, A. *J. Mater. Chem.* **2006**, *16*, 3099. (b) Wu, Y. L.; Liu, P.; Gardner, S.; Ong, B. S. *Chem. Mater.* **2005**, *17*, 221.
(47) Bauerle, P.; Pfau, F.; Schlupp, H.; Wurthner, F.; Gaudl, K.-U.; Caro, M. B.; Fischer, P. *J. Chem. Soc., Perkin. Trans. 2* **1993**, 489.
(48) Wei, Y.; Yang, Y.; Yeh, J.-M. *Chem. Mater.* **1996**, *8*, 2659.
(49) Seitz, D. E.; Lee, S. H.; Hanson, R. N.; Bottaro, J. C. *Synth. Commun.* **1983**, *13*, 121.
(50) Khor, E.; Ng, S. C.; Li, H. C.; Chai, S. *Heterocycles.* **1991**, *32*, 1805.
(51) Bauerle, P.; Fischer, T.; Bildlingmeier, B.; Rabe, J. P.; Stabel, A. *Angew. Chem., Int. Ed.* **1995**, *34*, 303.
(52) Bard, A. J.; Faulkner, L. A. *Electrochemical Methods - Fundamentals and Applications*; Wiley: New York 1984.
(53) Smith, K.; Barratt, M. L. *J. Org. Chem.* **2007**, *72*, 1031.
(54) Osaka, I.; Zhang, R.; Sauvé, G.; Smilgies, D.-M.; Kowalewski, T.; McCullough, R. D. *J. Am. Chem. Soc.* **2009**, *131*, 2521.
(55) Sonar, P.; Singh, S. P.; Leclère, P.; Surin, M.; Lazzaroni, R.; Lin, T. T.; Dodabalapur, A.; Sellinger, A. *J. Mater. Chem.* **2009**, *19*, 3228.
(56) Tsami, A.; Bunnagel, T. W.; Farrell, T.; Scharber, M.; Choulis, S. A.; Brabec, C. J.; Scherf, U. *J. Mater. Chem.* **2007**, *17*, 1353.
(57) Chen, T.-A.; Wu, X. M.; Rieke, R. D. *J. Am. Chem. Soc.* **1995**, *117*, 233.
(58) Faid, K.; Fréchette, M.; Ranger, M.; Mazerolle, L.; Lévesque, I.; Leclerc, M.; Chen, T.-A.; Rieke, R. D. *Chem. Mater.* **1995**, *7*, 1390.
(59) (a) Wei, Q.; Nishizawa, T.; Tajima, K.; Hashimoto, K. *Adv. Mater.* **2008**, *20*, 2211. (b) Kooistra, F. B.; Knol, J.; Kastenberg, F.; Popescu, L. M.; Verhees, W. J. H.; Kroon, J. M.; Hummelen, J. C. *Org. Lett.* **2007**, *9*, 551.
(60) Dimitrakopoulos, C. D.; Malenfant, P. R. L. *Adv. Mater.* **2002**, *14*, 99.
(61) Moulé, A. J.; Tsami, A.; Bunnagel, T. W.; Forster, M.; Kronenberg, N. M.; Scharber, M.; Koppe, M.; Morana, M.; Brabec, C. J.; Meerholz, K.; Scherf, U. *Chem. Mater.* **2008**, *20*, 4045.
(62) Wang, X. J.; Perzon, E.; Delgado, J. L.; de la Cruz, P.; Zhang, F. L.; Langa, F.; Andersson, M.; Inganas, O. *Appl. Phys. Lett.* **2004**, *85*, 5081.